Available online at www.sciencedirect.com
ScienceDirect
Developmental Biology 302 (2007) 195–207
DEVELOPMENTAL BIOLOGY
www.elsevier.com/locate/ydbio

Identification of interventricular septum precursor cells in the mouse embryo

Matthias Stadtfeld, Min Ye, Thomas Graf *

Department of Developmental and Molecular Biology, Albert Einstein College of Medicine, 1300 Morris Park Avenue Bronx, NY 10461, USA

Received for publication 28 July 2006; revised 8 September 2006; accepted 11 September 2006
Available online 16 September 2006

Abstract

Little is known about the formation of the interventricular septum (IVS), a central event during cardiogenesis. Here, we describe a novel population of myocardial progenitor cells in the primitive ventricle of the mouse embryo, which is characterized by expression of lysozyme M (lysM). Using LysM-Cre mice we show that lysozyme expressing cells give rise to the IVS and to a part of the left ventricular free wall, demonstrating that these heart regions are developmentally related. LysM+ precursors are not of hematopoietic origin and develop in the absence of transcription factors that regulate lysozyme expression in macrophages. LysM-deficient mice lack an overt cardiac phenotype, perhaps due to compensation by the related lysozyme P, which we also found to be expressed in the developing heart. Direct visualization of lysM expression, using LysM-EGFP knock-in mice, showed that ventricular septation is initiated at embryonic day 9 by the movement of myocardial trabeculae from the primitive ventricle towards the bulbo-ventricular groove and revealed the dynamics of IVS formation at later stages. Our studies predict that LysM-Cre mice will be useful to inactivate genes in the developing IVS.

Keywords: Lysozyme; Heart development; Interventricular septation; Lineage tracing; Heart morphogenesis; Cardiomyocytes

Introduction

The heart is the first organ that forms during mammalian development, satisfying the oxygen and nutrients needs of the growing embryo. The mature heart consists of two atria and two ventricles, the latter of which are separated by the interventricular septum (IVS). Ventricular septal defects are among the most common congenital heart lesions (Vaughan and Basson, 2000). Nevertheless, the knowledge about the origin of the IVS as well as of the dynamics and the control of its development remains sparse.

The first morphological evidence of cardiogenesis is the cardiac crescent, which forms in the mouse embryo at about embryonic day 7.5 (E7.5) from anterior mesoderm (Buckingham et al., 2005). Shortly thereafter the cardiac crescent fuses to give rise to the linear heart tube, which starts beating around E8, when extra-embryonic and embryonic vascular networks amalgamate (McGrath et al., 2003). The heart tube undergoes complex remodeling processes during midgestation to form the four-chambered adult organ. During the initial remodeling steps between E8.5 and E10.5, the cardiac chambers become evident as a consequence of the forward looping of the posterior parts of the heart tube and the thickening of the myocardium (Buckingham et al., 2005). The chambers then get physically separated by the growth of the septae and valves, thereby allowing for directed flow of the blood stream. The developing heart is subdivided by the formation of the IVS, which is located between the left and right ventricles. IVS formation in the mouse occurs approximately between E11 and E12.5 and involves the recruitment of myocardial cells as well as of non-muscular mesenchymal cells (Kaufman and Bard, 1999).

Dye injection experiments in chicken embryos showed that cardiomyocytes in the IVS are derived from the region of the bulbo-ventricular groove (de la Cruz et al., 1997). This structure demarcates the separation between the embryonic left and right ventricle and becomes detectable at about E10 in the mouse embryo. The analysis of staged chicken embryos suggested that the IVS forms by the coalescence of individual muscle fiber bundles – so-called trabeculae – present in the primitive left ventricle (Ben-Shachar et al., 1985). However, this study did not

* Corresponding author. Fax: +1 718 430 3305.
E-mail address: graf@aecom.yu.edu (T. Graf).

0012-1606/$ - see front matter © 2006 Elsevier Inc. All rights reserved.
doi:10.1016/j.ydbio.2006.09.025

address where IVS precursors reside prior to formation of the bulbo-ventricular groove. Elegant lineage tracing experiments in the mouse indicate that the myocardium of the IVS has a dual origin, being derived partly from the right and partly from the left ventricular primordium (Meilhac et al., 2004). A number of genes have been implicated in IVS formation. Thus, mice with targeted deletions of the transcription factors Tbx5 (Takeuchi et al., 2003) and SRF (Parlakian et al., 2004) as well as of the chemokine receptor CXCR4 (Tachibana et al., 1998; Zou et al., 1998) and its ligand SDF-1 (Nagasawa et al., 1996) all have ventricular septal defects. However, because specific gene ablation in the IVS is not yet possible it cannot be ruled out that the observed phenotypes are secondary to one of the many cardiac and systemic abnormalities in these animals.

Lysozyme is a bacteriolytic enzyme that is part of the innate immune system. Mice have two closely related lysozyme genes: LysM (*Lyzs*, called *lysM* in the following), which is expressed in macrophages and granulocytes (Cross et al., 1988) as well as type II alveolar epithelial cells in the lung (Rehm et al., 1991). And lysP (*Lzp-s*, called here *lysP*), which is expressed in the Paneth cells of the small intestine (Cross et al., 1988). Here, we report the surprising finding that lysM is also expressed transiently in a novel population of myocardial precursors of the IVS. The study of a mouse model with a knock-in of *egfp* into the endogenous *lysM* locus (Faust et al., 2000) allowed us to directly visualize the dynamics of IVS formation. In addition, we traced the developmental fate of lysM+ myocardial cells by Cre/loxP technology. Our study shows that IVS precursors are determined before septation is initiated and that the muscular compartment of the IVS is derived from at least two types of progenitor cells. In addition, our work suggests that cardiac-specific mechanisms of lysozyme regulation exist and that this enzyme has hitherto unknown functions in the heart.

Materials and methods

Mice

LysM ancestry (Ye et al., 2003) and LysM-EGFP (Faust et al., 2000) mice were used as homozygotes for the LysM-Cre and LysM-EGFP alleles, respectively. Vav ancestry mice (Stadtfeld and Graf, 2005) were heterozygous for vav-Cre. LysM ancestry mice were homozygous for ROSA26R-YFP or ROSA26R-lacZ (Soriano, 1999; Srinivas et al., 2001), respectively. Lysozyme ancestry mice lacking PU.1 were obtained by crossing them for two generations to animals heterozygous for a germ line deletion of PU.1 (Ye et al., 2005). Similarly, LysM-EGFP mice lacking C/EBPβ were generated by crossed them with C/EBPβ mutant mice (Sterneck et al., 1997). All genotyping was performed as previously described (see above references). Mice were bred and maintained in accordance with guidelines from the Institute for Animal Studies of the Albert Einstein College of Medicine.

X-gal and EGFP whole mounts

For X-gal whole mounts of adult hearts, mice were anesthetized with isoflurane and perfused into the left ventricle with PBS followed by 1.5% paraformaldehyde (PFA, Electron Microscope Science), before hearts were dissected and fixed in 1.5% PFA overnight at 4°C. Fixed hearts were incubated in X-gal staining solution containing 1 mg/ml of X-gal (5-bromo-4-chloro-3-indolyl-βD-galactoside, FisherBiotech) in 2 mM $MgCl_2$, 5 mM $K_3Fe(CN)_6$, 5 mM $K_4Fe(CN)_6$ and 0.02% NP40 in PBS, pH 7.4 for 12–24 h in the dark at 37°C. Imaging was done using a Nikon SMZ 1500 dissection microscope equipped with an Insight FireWire camera and SPOT imaging software (Diagnostic Instruments). To render hearts transparent they were dehydrated through a methanol series followed by incubation in a 2:1 mixture of benzyl benzoate: benzyl alcohol (Rentschler et al., 2001).

For EGFP whole mounts of the developing heart embryos were obtained from timed matings with the noon of the day of the vaginal plug designated embryonic day 0.5 (E0.5). The developmental stage was verified by counting somite pairs (between E8.5 and E11.5) or by other morphological criteria (Downs and Davies, 1993). Embryonic hearts were isolated with microdissection tweezers (Roboz Surgical) by clipping the distal part of the outflow tract and the two horns of the sinus venosus. For EGFP visualization, hearts were mounted in a drop of PBS and imaged with a Nikon Eclipse E600 microscope equipped with a FITC filter (Chroma #41001) and a MagnaFire (Optronics, Goleta, CA) camera. Image processing was done in Adobe Photoshop.

Preparation and analysis of frozen sections

Anesthetized adult mice were perfused into the left ventricle with PBS followed by 4% PFA. Dissected hearts were fixed in 1.5% PFA containing 30% sucrose for 1 h at 4°C, then they were cut in half and incubated for another 8–12 h in the fixation solution. Embryos and newborn mice were fixed as a whole for 6 h to overnight, depending on the developmental stage. For embryos older than E12.5, the head was removed to allow better penetration of the fixative. Tissues were embedded in O.C.T. compound (Sakura, Torrance, CA) and submerged in 2-methylbutane at −80°C. 10-μm sections were cut using a Leica CM1900 cryostat, transferred onto pre-cleaned glass slides (Superfrost/Plus, Fisher Scientific) and stored at −80°C.

Immunofluorescence was performed using the M.O.M. basic kit (Vector Labs, Burlingame, CA) following the manufacturer's instructions with the additional inclusion of 0.3% Triton-100 in all solutions and of 3% BSA and 5% goat serum in the blocking solution. Antibodies used were mouse-monoclonal anti α-actinin (Sigma) followed by an Alexa Fluor 546®-conjugated goat anti-mouse antibody (Invitrogen) as well as APC-conjugated rat monoclonal antibodies against mouse CD31, CD45, Mac-1, Gr1 (Pharmingen) and F4/80 (Caltag, Burlingame, CA). GFP and YFP signals were sometimes amplified using an Alexa Fluor 488®-conjugated rabbit anti-GFP antibody (Invitrogen). DAPI (0.4 μg/ml) was included to visualize nuclei. Sections were observed under a Nikon Eclipse E600 microscope equipped with filters to visualize DAPI (Chroma #31000), GFP or Alexa Fluor® 488 (Chroma #41001), YFP (Chroma #41028), Alexa Fluor® 546 (Chroma #41002c) and APC (Chroma #41013). Images were taken using a MagnaFire camera (Optronics) and analyzed with Adobe Photoshop software. For the calculation of the proportion of reporter labeled cardiomyocytes in vav ancestry mice it was assumed that the adult murine heart contains a total of 1.9×10^6 cardiomyocytes (Brodsky et al., 1985). Sections containing 10,000 to 50,000 cardiomyocytes were analyzed per vav ancestry mouse.

Real-time PCR analysis

Hearts were dissected from E9.5 (19–24 somite pairs) LysM-EGFP and C57BL/6 embryos and common atrial chamber, outflow tract and large parts of the bulbus cordis were dissected away. Repeated washing steps removed contaminating maternal and embryonic blood cells. RNA was extracted from pools of 3–5 hearts using the QIAGEN RNeasy Micro Kit following the manufacturers' instructions. Reverse transcription was done with the iSelect cDNA Synthesis Kit (Bio-Rad) and real-time PCR reactions were performed in triplicates with an Opticon2 (MJ Research) using AmpliTag Gold (Roche) and SybrGreen (Applied Biosystems). The input cDNA amount for each reaction was equivalent to 1/20 to 1/10 of one dissected embryonic heart. The following primer pairs were used: 5′-GGAATGGCTGGCTACTATGG-3′ and 5′-TGCTCTCGTGCTGAGCTAAA-3′ (lysM), 5′-ATGGCTACCGTGGTGT-CAAG-3′ and 5-CGGTCTCCACGGTTGTAGTT-3′ (lysP), and 5′-GACGGC-CAGGTCATCACTATTG-3′ and 5′-AGGAAGGCTGGAAAAGAGCC-3′ (β-actin). The PCR efficiency with all primer pairs was >90%. Specificity of lysM and lysP detection was tested by digestion of the PCR products with HaeIII, which only cuts lysM.

Results

A subset of adult cardiomyocytes is derived from lysM expressing cells

To trace the developmental fate of hematopoietic cells of the granulocyte/macrophage lineage we used mice with a knock-in of Cre recombinase into the endogenous lysM locus (Clausen et al., 1999). These mice were crossed with two conditional reporter mouse strains (Soriano, 1999; Srinivas et al., 2001). In the resulting LysM ancestry mice the progeny of lysozyme expressing cells are irreversibly labeled by either yellow-fluorescent protein (YFP) or β-galactosidase (β-gal) (Fig. 1A). As expected, LysM ancestry mice showed reporter gene expression in essentially all granulocytes and monocytes (Ye et al., 2003) as well as in tissue macrophages and lung epithelial cells (data not shown).

A detailed examination of LysM ancestry mice with the *lacZ* reporter gene by whole-mount X-gal staining surprisingly revealed that large parts of the heart muscle were reporter-positive (Fig. 1B). The pattern of labeling in the cardiac whole mounts showed the highest density in the vertical midline, where the IVS is located. From there the labeling extended both into the anterior and posterior side of the left ventricular free wall while the atria, the right ventricle as well as the distal part of the left ventricular free wall were negative (Fig. 1B and data not shown). Analysis of serial heart sections showed the presence of reporter labeled cells with the morphology of

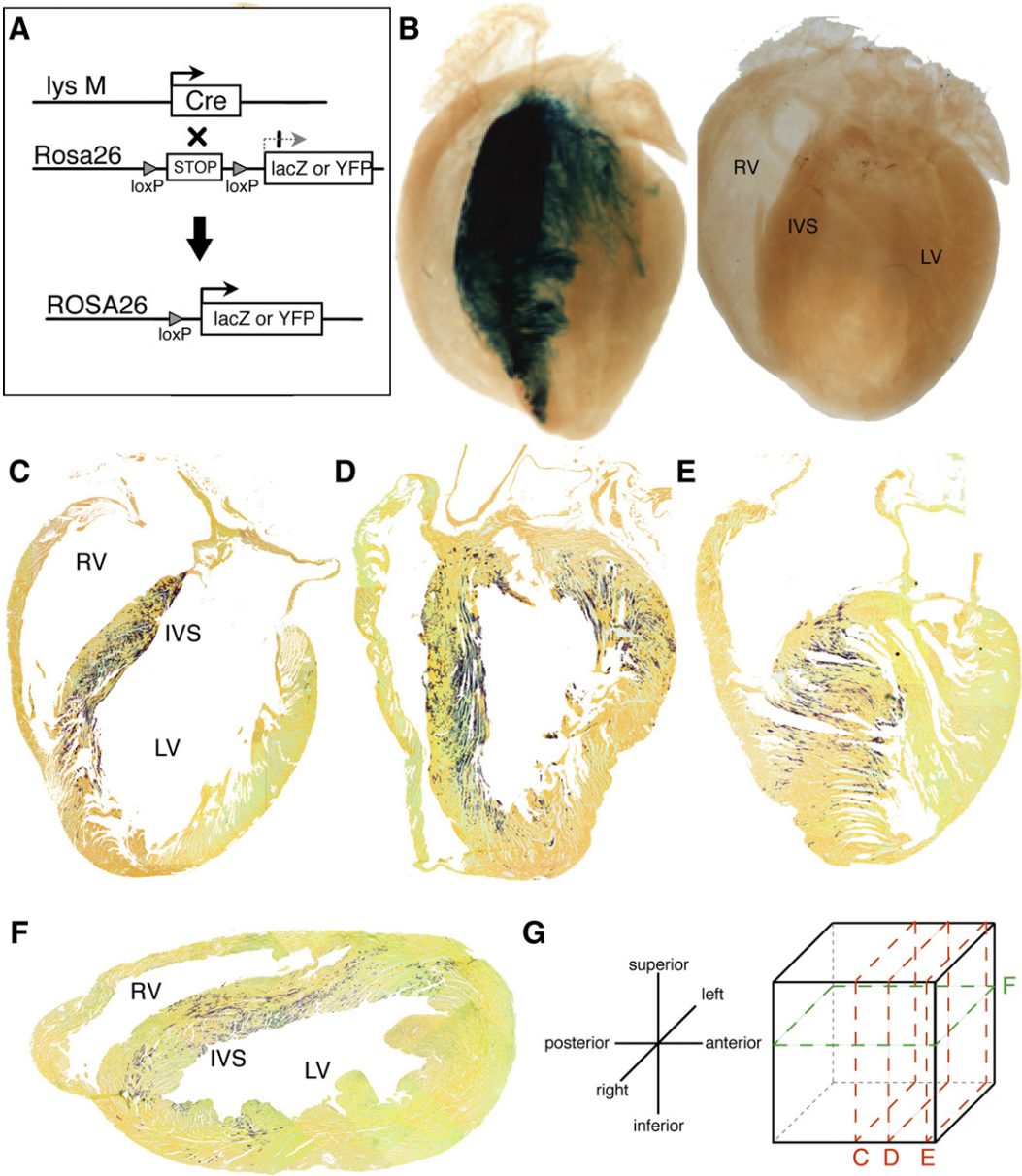

Fig. 1. X-gal labeling in the heart of adult LysM ancestry mice. (A) Breeding scheme to generate LysM ancestry mice, which allow tracing of the progeny of lysM expressing cells. (B) X-gal stained whole mounts of hearts from an adult LysM ancestry (left) and a ROSA26R-lacZ mouse used as negative control (right). IVS, interventricular septum; LV, left ventricle; RV, right ventricle. (C–E) X-gal stained sections through hearts of LysM ancestry mice in coronal and (F) transverse orientation. Note the complete absence of reporter labeled cardiomyocytes in the right ventricle and atria. (G) Scheme to illustrate the planes of sectioning in panels C–F.

cardiomyocytes along the entire length of the IVS, with a higher prevalence in the part of the myocardium that faces the lumen of the left ventricle (Fig. 1C). Anteriorly and posteriorly from the midline, reporter labeled cells were also found in the left ventricular free wall, especially towards the base of the heart (Fig. 1D). Longitudinal sections close to the anterior and posterior ends of the heart muscle showed that reporter labeling marked the extension of the IVS into this region (Fig. 1E). Cross-sections further confirmed the total absence of labeled cardiomyocytes in the right ventricle and the distal end of the left ventricular free wall (Fig. 1F).

To better characterize the reporter gene expressing cells, we analyzed heart sections of adult LysM ancestry mice using e*yfp* as a reporter gene. This showed that large numbers of interventricular cardiomyocytes, identified by their morphology and the expression of the muscle marker α-actinin, were indeed YFP labeled (Figs. 2A–E). In addition to their mentioned asymmetric distribution in the IVS, reporter labeled cardiomyocytes often formed clusters of muscle fibers that showed a different orientation than neighboring reporter-negative cardiomyocytes (Fig. 2A). This indicates that these cells are distinct developmental and/or functional units of the heart muscle. YFP+ cardiomyocytes were negative for the macrophage markers CD45, F4/80, Mac-1 and Gr1 (Figs. 2C–E) and the endothelial marker CD31 (data not shown). No GFP expression was detected in cardiomyocytes of adult LysM-EGFP mice (Figs. 2F, G), demonstrating that lysM is not expressed in these cells.

Interventricular cardiomyocytes are not derived from hematopoietic cells

We next addressed whether the labeling seen in LysM ancestry mice results from hematopoietic-to-cardiac conversions, which have been reported to occur at high frequency after bone marrow transplantation into adult recipients (Orlic et al., 2001). Such conversions remain highly controversial (Balsam et al., 2004; Murry et al., 2004). To this end we analyzed the hearts of vav ancestry mice, in which essentially all hematopoietic cells, including stem and progenitor cells, are irreversibly labeled both in embryos and in adults and therefore can be traced (Stadtfeld and Graf, 2005). In these mice no macroscopically detectable reporter gene labeled cardiomyocytes were detected in the IVS or in any other heart region (Suppl. Fig. 1A). Nevertheless, analysis of frozen sections revealed that 1:5000 to 1:2000 cardiomyocytes are YFP+ in vav ancestry mice (Suppl. Figs. 1B–D). These cells were not confined to a particular region of the myocardium. Together, these observations show that the labeled cardiomyocytes in the hearts of LysM ancestry mice are not of hematopoietic origin, but raise the possibility that rare hematopoietic-to-cardiomyocyte conversions occur.

As expected, CD45+Mac-1+ hematopoietic cells present in the heart muscle of LysM ancestry mice were also YFP labeled (Fig. 2E). These cells, which actively expressed lysM as well as the CSF-1 receptor (Fig. 2F and data not shown), were found throughout the heart in surprisingly high numbers, most abundantly in the atria and the inner surface of the ventricular chambers (Suppl. Fig. 2). Strikingly, in the IVS and the ventricle walls, these tissue macrophages were organized in a parallel fashion to cardiomyocytes, often directly overlying them (Fig. 2F and Suppl. Fig. 2D). Similar cells were also reporter labeled in vav ancestry mice (data not shown).

Myocardial precursor cells express lysM in the embryonic heart

To determine when during heart development lysM is expressed, we analyzed LysM-EGFP embryos at different developmental stages by whole-mount fluorescence microscopy. No GFP expression could be detected up to embryonic day E8.5 (10–12 somite stage) (data not shown). However, at E9.5 strong GFP fluorescence was seen in the heart while no GFP+ hematopoietic cells were present in circulation or the liver rudiment (Figs. 3A, B). Imaging of dissected hearts between E9 and E9.5 showed that GFP+ cells initially (15 somite stage) formed an almost continuous ring that was perpendicular to the anterior–posterior axis of the heart tube. Soon thereafter (19 somite stage) two domains of strong GFP expression became visible within this ring: a dorsal domain close to the outflow tract and the common atrial chamber and a ventral domain, extending from the forming bulbo-ventricular groove into the primitive ventricle (Figs. 3C–E). Sections through an E10 embryo (25 somite stage) showed that GFP+ cells localized to muscular protrusions of the heart muscle, so called trabeculae, in the primitive ventricle (Figs. 3F–H). No GFP+ cells were seen in other regions of the developing heart. Immunofluorescence staining on sections of an E9 (17 somite stage) embryo showed that all GFP+ cells present in the heart expressed the muscle marker α-actinin (Fig. 4) while none of them expressed the endothelial marker CD31 or the hematopoietic markers CD45, Mac-1 and F4/80 (data not shown). These results show that a subset of myocardial cells in the mouse embryo express lysM.

Lysozyme expression reveals dynamics of IVS formation

To follow the dynamics of cardiac lysozyme expression we analyzed hearts from E10.5, E11.5 and E13.5 embryos by whole-mount fluorescence microscopy. At E10.5, the ring of GFP+ cells extending into the primitive ventricle and its two domains of GFP expression were still visible (Fig. 5A). However, compared to E9 (see Fig. 3) the fluorescence intensity of the ventral domain had increased while that of the dorsal domain had decreased. This trend continued at E11.5, when expression in the dorsal domain was almost extinguished and the ventral domain extended dorsally, visualizing the closure of the interventricular foramen by the myocardial component of the IVS (Fig. 5B). At E13.5, when septation is complete, myocardial lysozyme expression formed a brightly fluorescent "zipper" between the right and left ventricle, highlighting the position of the IVS (Fig. 5C). An artistic rendering of these processes summarizes the dynamics of lysM expression in the developing heart (Fig. 5, right panel).

To analyze IVS development after E13.5, when the heart becomes too opaque for whole-mount fluorescent microscopy,

we analyzed frozen sections from crosses between LysM-EGFP and LysM ancestry mice. This permitted the simultaneous visualization of both past and ongoing lysM expression. As shown in Fig. 6, at E14.5 GFP expression was strongest in the tip and outer layers of the IVS as well as in trabeculae of the left ventricle close to the base of the IVS. Essentially all GFP+ cells were also X-gal+ (compare Figs. 6D and E). This indicates that activation of the *lysM* locus was not a very recent event in these cells since Cre expression is not immediately translated into detectable reporter activation X-gal+ GFP− cardiomyocytes, which previously had expressed lysozyme but did not maintain this expression, were also present. However, they localized to different parts of the myocardium than cardiomyocytes that still actively expressed lysozyme: The dorsal region of the heart separated from the growth area of the IVS by a buffer of X-gal-negative mesenchymal cells (region I, Figs. 6B, C) and the

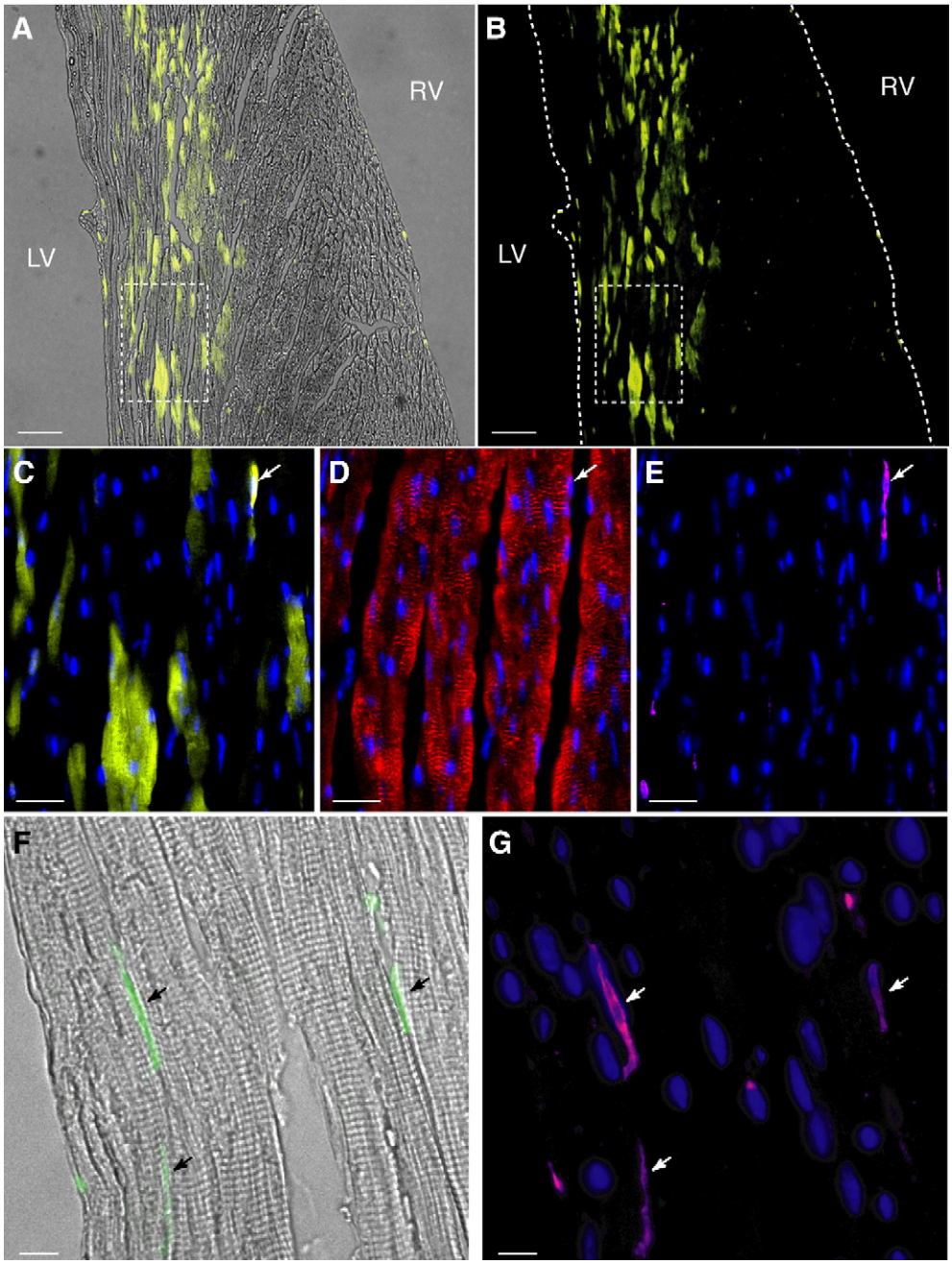

Fig. 2. Reporter labeling in heart sections of adult LysM ancestry and LysM-EGFP mice. (A–E) Coronal sections through the IVS of a LysM ancestry mouse, with YFP fluorescence in yellow, α-actinin in red, CD45 in purple and DAPI in blue. (A, B) Overlay of YFP and brightfield (A) and YFP fluorescence only (B). Scale bar = 50 μm. YFP labeled cardiomyocytes are mostly seen on the left side of the IVS. Note also that all YFP+ fibers run parallel to the plane of sectioning while most YFP− fibers are oriented perpendicular to it. (C–E) Magnification of the area boxed in panels A and B, demonstrating co-expression of YFP and α-actinin. Overlays of DAPI and YFP (C), DAPI and α-actinin (D) and DAPI and CD45 (E). An arrow highlights an YFP^+ $CD45^+$ hematopoietic cell. Scale bar = 15 μm. (F, G) Section through the IVS of a LysM-EGFP mouse showing overlays of GFP (green) and brightfield and DAPI and CD45, respectively. Arrows indicate GFP+ $CD45^+$ macrophages. Scale bar = 15 μm. Note that cardiomyocytes are GFP-negative.

compact center of the IVS (region II, Figs. 6D, E). In newborn mice lysM expression was still detectable within a thin layer of cardiomyocytes surrounding the superior part of the IVS, and became undetectable after the second postnatal week (data not shown). Together, these observations show that after ventricular septation is completed lysozyme expressions continues to be dynamically expressed in the IVS.

LysP is also expressed in the embryonic heart

We next determined whether lysP, which shows >90% identity to lysM at the amino acid level, is also expressed in the developing heart. To this end we performed quantitative real-time PCR on cDNA prepared from E9.5 primitive ventricle. At this stage lysozyme expression is not detectable in circulating

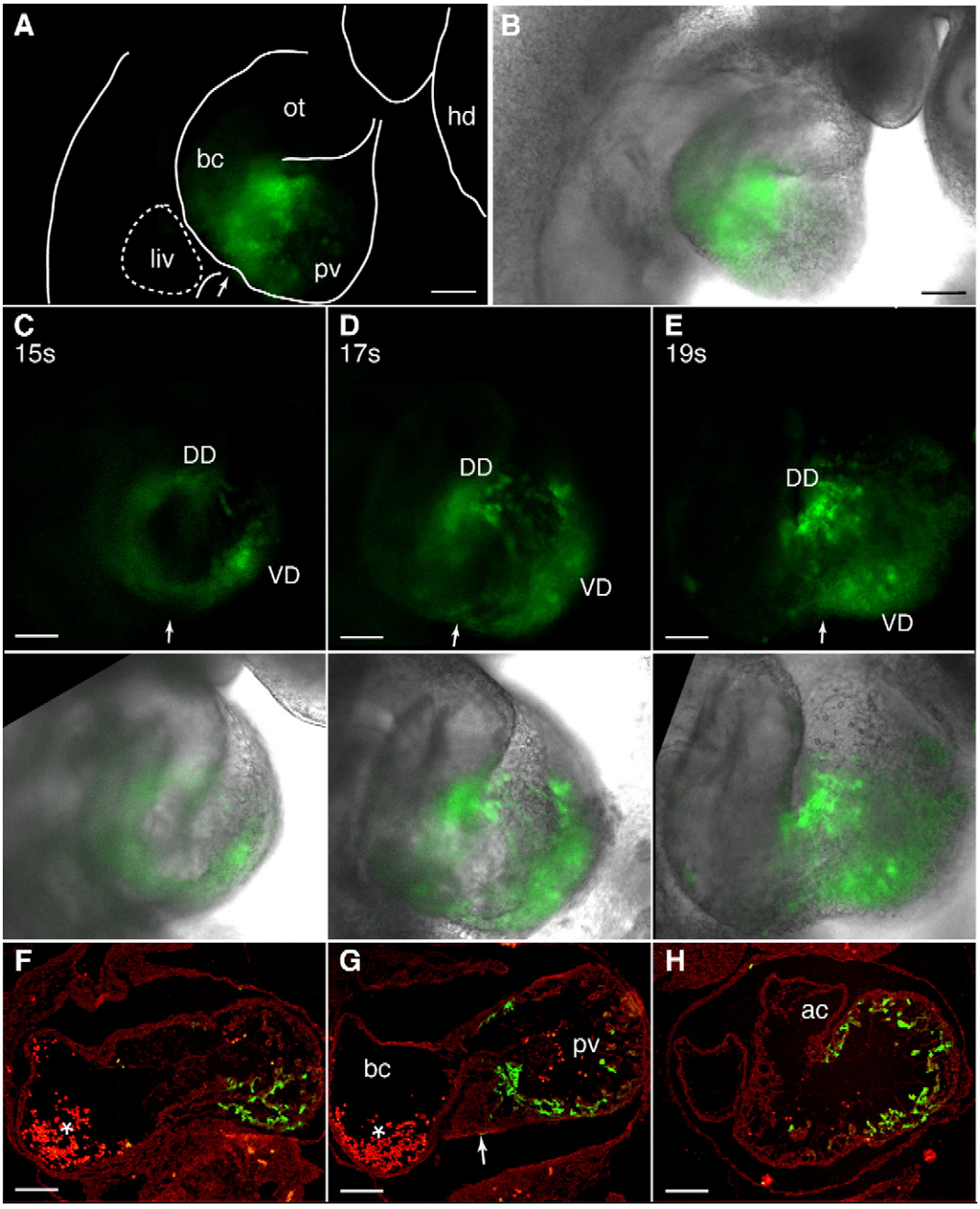

Fig. 3. GFP fluorescence in the heart of LysM-EGFP embryos. (A, B) Images showing GFP fluorescence in an E9.5 LysM-EGFP embryo without (A) and with (B) an overlaying brightfield image. The position of the liver rudiment (liv) is outlined by a dotted line. ac, Common atrial chamber; hd, head and ot, outflow tract. Scale bar=250 μm. (C–E) Fluorescent images of hearts from three E9 LysM-EGFP embryos at different somite pair stages (15 s, 17 s and 19 s). The lower rows show overlays of GFP and brightfield images. The arrows indicate the location of the nascent bulbo-ventricular groove. The dorsal (DD) and ventral (VD) domains of GFP expression are indicated. Scale bar=100 μm. (F–H) Frozen sections in transverse orientation of an E10 (25 s) embryo. GFP fluorescence in green, autofluorescence in red. The dorsal side of the embryo is facing up. Sections move anteriorly from panels F to G. The arrow indicates the location of the nascent bulbo-ventricular groove and the asterisks accumulations of red blood cells in the bulbus cordis (bc). Scale bar=60 μm. Note that the GFP labeling is restricted to trabeculae in the primitive ventricle (pv).

hematopoietic cells nor in tissue macrophages (Lichanska et al., 1999) (see also Figs. 3A, B). This analysis revealed that lysP is expressed in the developing heart at levels similar to lysM both in wild type and in lysM-deficient mice (Fig. 7A). In contrast, in bone marrow lysP expression is only detectable in the absence of lysM (Fig. 7B). The observed ~50 fold difference in expression of lysM in the two tissues examined represents an overestimate since the percentage of lysozyme expressing cells is lower in the E9.5 heart (<5%) than in the bone marrow (60–70%). These results show that both lysM and lysP genes are expressed in the heart of E9.5 embryos while lysM but not lysP is expressed in hematopoietic cells.

Cardiac lysM expression does not require PU.1 and C/EBPβ

The expression of *lysM* in macrophages is controlled by the PU.1 and C/EBPβ (Faust et al., 1999; Lefevre et al., 2003). To test whether cardiac lysM expression is similarly regulated we crossed LysM ancestry with animals containing a targeted deletion of PU.1 (Ye et al., 2005) and analyzed newborn pups of the F2 generation by X-gal staining. This revealed no differences between wild type and homozygous mutant animals with respect to the abundance and organization of labeled cardiomyocytes (Suppl. Figs. 3A–B). As expected, X-gal+ hematopoietic cells were abundant in the liver of wild type mice but totally absent in the PU.1 knockout animals (Suppl. Figs. 3C–D). Similarly, E11 LysM-EGFP embryos lacking C/EBPβ showed no reduction in cardiac GFP labeling, while lysozyme expression in fetal liver macrophages was significantly lowered (Suppl. Figs. 3E–G).

Discussion

LysM expression defines a novel cardiac progenitor population of non-hematopoietic origin

Here, we report the unexpected finding that lysM marks a subset of embryonic myocardial precursors that form large parts of the interventricular septum as well as portions of the left ventricle in the adult heart (Fig. 1, see also scheme in Fig. 8). While lysM is best known for its expression in macrophages, cardiomyocytes derived from lysM expressing cells are not of hematopoietic origin. Thus, regions of the heart that are strongly labeled in LysM ancestry mice are mostly negative in vav ancestry mice (Suppl. Fig. 1), a model that traces all hematopoietic lineages and shows an earlier onset of blood

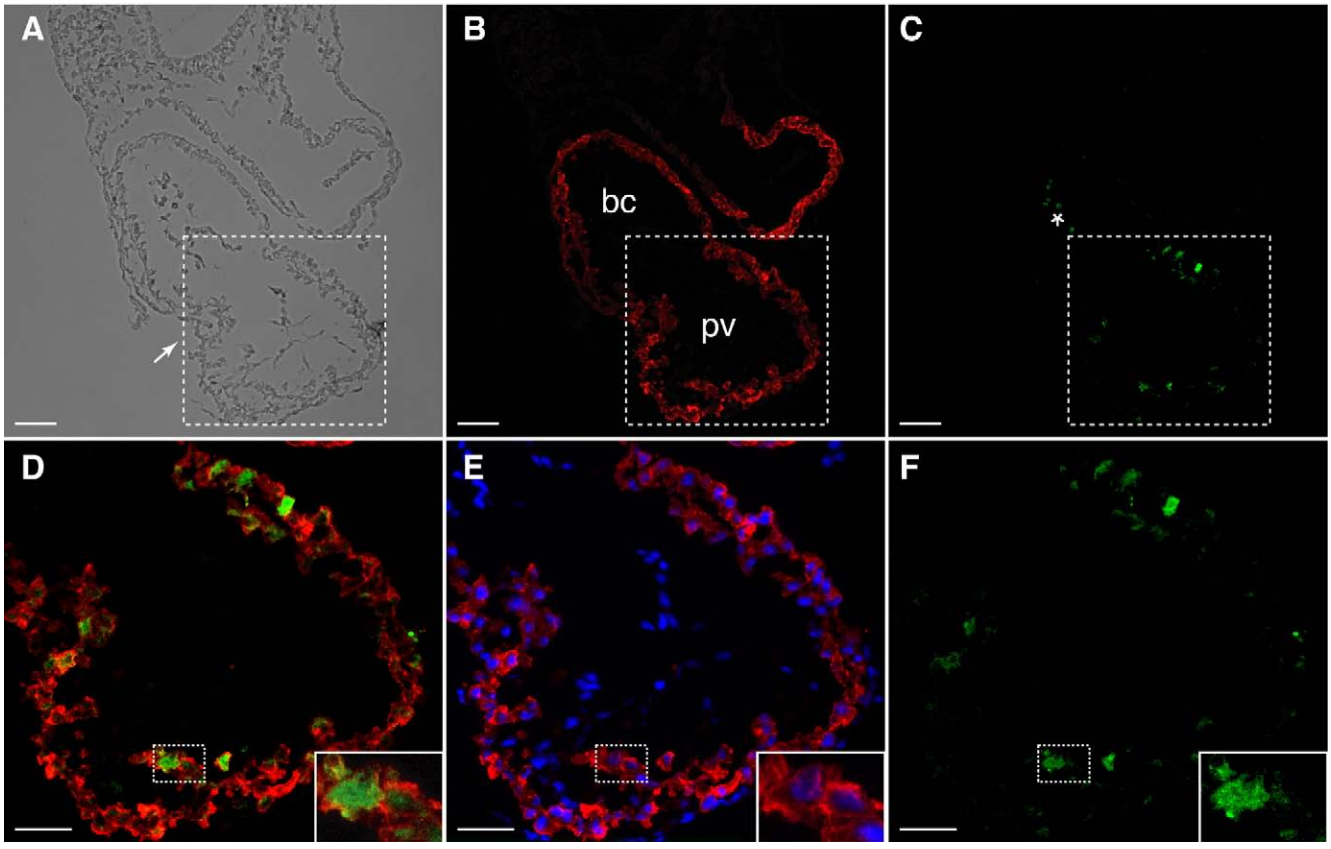

Fig. 4. Myocardial nature of lysozyme expressing cells in the heart of LysM-EGFP embryos. (A–C) Frozen section through the heart of an E9.5 LysM-EGFP embryo showing GFP fluorescence (green) and staining for α-actinin (red). The arrow in panel A indicates the position of the forming bulbo-ventricular groove and the asterisk in panel C circulating autofluorescent red blood cells. Scale bar = 100 μm. (D–F) Magnification of area boxed in panels A–C showing overlays of GFP and α-actinin (D), α-actinin and DAPI (blue, E) and GFP fluorescence only (F). Staining with the hematopoietic markers CD45, Mac-1 and F4/80 gave no detectable signals. Note that GFP expression is restricted to cells that express α-actinin. The inserts in panels D–F show a magnified view of a GFP+ and a GFP− myocardial cell (boxed area). Scale bar = 50 μm.

cell labeling than LysM ancestry mice (Stadtfeld and Graf, 2005). The rare reporter-positive cardiomyocytes (1:5000 to 1:2000) in vav ancestry mice might reflect inappropriate expression of vavCre in cardiomyocytes (or their precursors), although a hematopoietic origin of the labeled cells cannot be excluded. The observed frequency of labeled cardiomyocytes in these mice therefore represents the upper limit of possible hematopoietic-to-cardiomyocyte conversions during normal development.

The myocardial identity of the lysozyme expressing cells in the developing heart was shown by α-actinin expression and the cells' morphology, which was indistinguishable from surrounding lysM− cardiomyocytes (Figs. 4D–F). The position of lysM+ cells within the embryonic heart and their contribution to specific regions of the adult heart establishes them as a novel population of cardiac precursors. This conclusion is supported by the pattern of reporter gene expression in LysM-EGFP embryos, which differs from that of more than a dozen

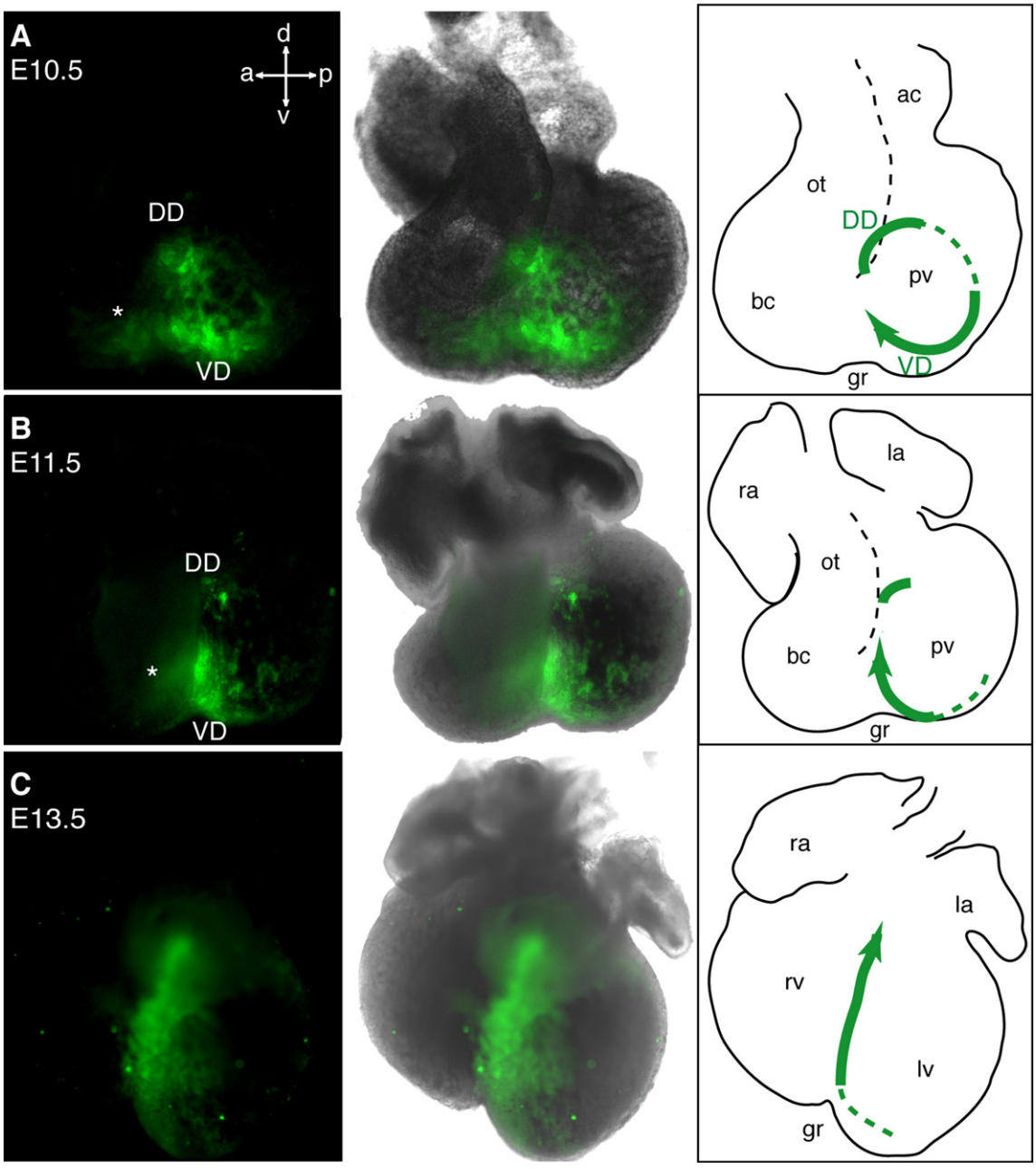

Fig. 5. Dynamics of IVS formation as delineated by lysozyme expression. Images of entire hearts dissected from LysM-EGFP embryos at E10.5 (A), E11.5 (B) and E13.5 (C) showing GFP fluorescence (green, left panels), overlay of GFP and brightfield (middle panels) as well as schematics interpreting the images (right panels). The green line and the arrow indicate the location of GFP+ cells and their probable movements, while the broken line indicates regions where GFP+ cells were detected at an earlier stage. Anterior (a), posterior (p), dorsal (d) and ventral (v) orientations are indicated by the cross. ac, Atrial chamber; ot, outflow tract; bc, bulbus cordis; pv, primitive ventricle; gr, bulbo ventricular groove; la, left atrium; right atrium ra; lv, left ventricle and rv, right ventricle. Note that GFP fluorescence is largely restricted to the primitive ventricle except for a weak signal originating at E10.5 from the region of the bulbus cordis (asterisk). The significance of this signal is unclear since it has not been verified in sections of the same region.

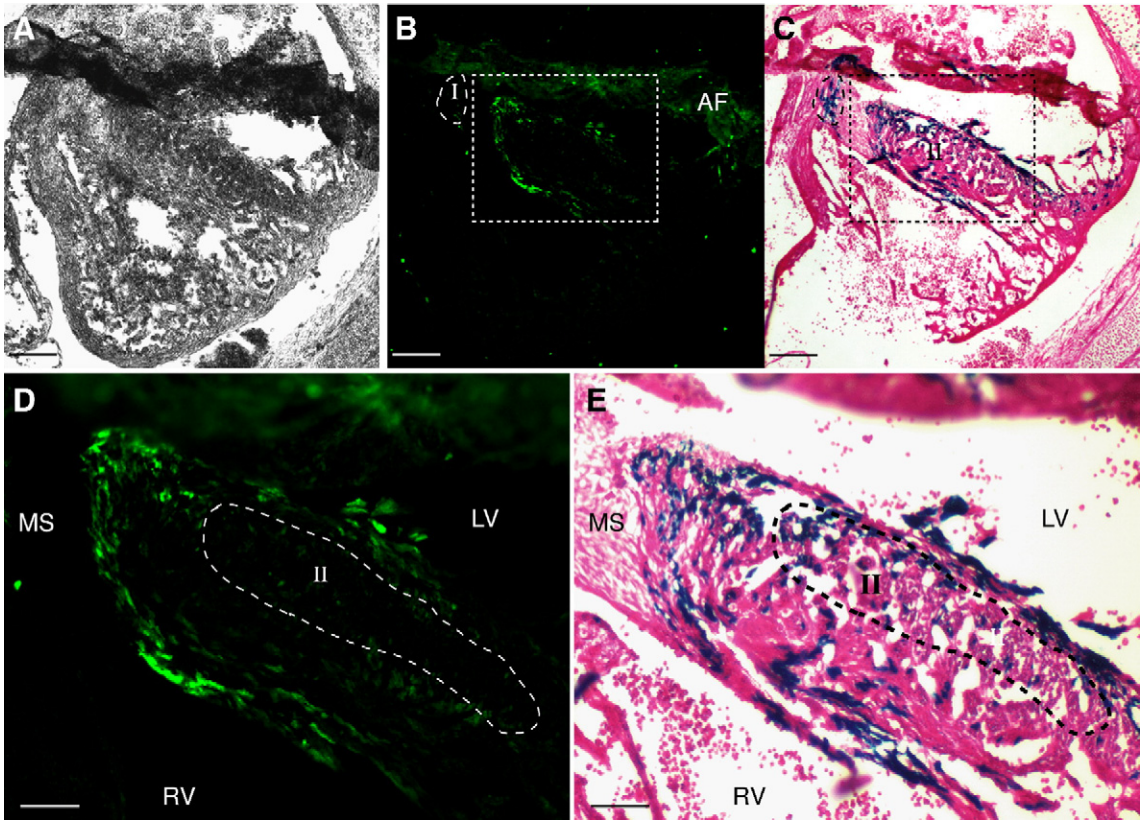

Fig. 6. Dynamics of lysozyme expression during late stages of IVS formation. (A–C) Transverse section through the heart of an E14.5 LysM-EGFP × LysM *lacZ* ancestry mouse imaged in brightfield illumination (A), for GFP fluorescence before X-gal staining (B) and in brightfield after X-gal staining (C). The dorsal heart region, where lysM was previously expressed, is outlined and labeled as 'I'. The signals seen in the upper part of panel (B) represent autofluorescence (AF) due to tissue compaction during preparation of the section. Scale bar=250 μm. (D, E) Magnification of area boxed in panels B and C. The outline of a region labeled 'II' indicates the position of X-gal+ GFP− cells in the inner myocardium of the IVS, where lysM expression is not maintained. Note the presence of a buffer of mesenchymal cells (ms) between X-gal+ cells within the IVS and a group of dorsally located X-gal+ cells. Scale bar=100 μm.

transgenic reporter mice with different cardiac-specific promoters (Habets et al., 2003). The domain of lysozyme expression is also distinct from the cardiac conduction system (Rentschler et al., 2001), although it is possible that some of the cardiomyocytes labeled in LysM ancestry mice are part of the IVS component of this system. With respect to known cardiac precursor populations, the localization of lysM+ cells to the primitive ventricle at E9 precursors suggests that these cells are a subset of the primary heart field, which is believed to be the exclusive source of myocardial cells in this structure left ventricle at this stage (Buckingham et al., 2005). On the other hand, a recent study using transgenic mice with Cre recombinase controlled by regulatory elements of the *mef2C* gene indicated that the entire IVS is derived from the secondary heart field, which also forms the right ventricle and the outflow tract (Verzi et al., 2005). This apparent contradiction can be resolved when assuming that the part of the primitive ventricle that gives rise to the IVS is in fact derived from the secondary

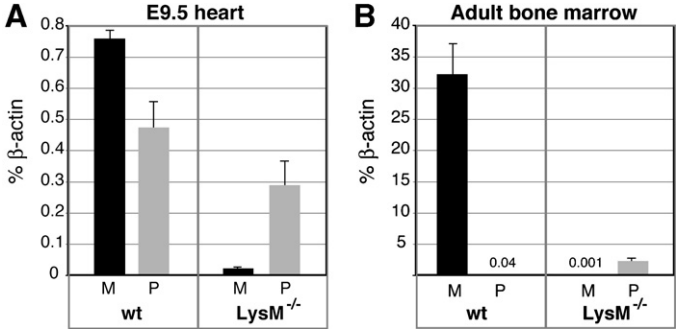

Fig. 7. LysM and lysP expression in the developing heart. The expression levels of lysM and lysP in E9.5 hearts (A) and adult bone marrow (B) of lysM-deficient LysM-EGFP$^{ki/ki}$ and wild type (wt) mice were determined by quantitative real-time PCR analysis relative to β-actin. Error bars indicate the range of two independent experiments, each using RNA isolated from 3–5 embryos and 2–3 adult mice, respectively.

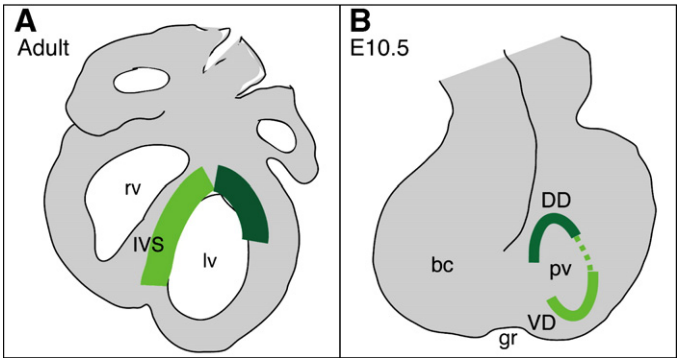

Fig. 8. Summary diagram. (A) The drawing represents a para-sagittal section through an adult heart, with structures derived from the ventral and dorsal embryonic domains of lysM expression indicated in light and dark green, respectively. (B) Representation of a whole mount of an E10.5 heart showing the ring of lysozyme expressing cells. The ventral domain (VD) and the dorsal domain (DD) of lysozyme expressing cells are highlighted in light and dark green, respectively, which contain the precursors of the corresponding color coded domains in panel A. The discontinuity within the ring seen at later developmental stages is indicated by the dotted line. bc, Bulbus cordis; gr, bulbo-ventricular groove; IVS, interventricular septum; lv, left ventricle; pv, primitive ventricle and rv, right ventricle.

and not the primary heart field. Our observation that lysM+ cells contribute to the IVS but only little to the outer muscular layers of left ventricle or the left ventricular freewall (see Fig. 1), also suggests that septum and ventricle are derived from two different primordia. Thus, lysM+ ventricular precursor cells do not take part in the ballooning out that will give the left ventricle its ultimate shape (Moorman and Christoffels, 2003). In the developing human heart a population of myocardial cells expressing the neuronal antigen G1N2 have been described that surround the interventricular foramen in a similar fashion as lysM+ cells (Lamers et al., 1992; Wessels et al., 1992) (see also Fig. 5A). These cells might represent the human counterparts of the murine cardiac progenitors described by us.

Dynamics of IVS formation

The tracing of lysozyme-positive cells by GFP expression revealed the presence of labeled myocardial cells at E9, before the initiation of ventricular septation and the formation of the bulbo-ventricular groove. Thus, the IVS primordium is specified earlier than hitherto appreciated (de la Cruz et al., 1997; Kaufman and Bard, 1999).

Based on the analysis of staged LysM-EGFP embryos, the first step of IVS morphogenesis consists of an anterior movement of cells from the primitive ventricle, leading to their accumulation in the nascent bulbo-ventricular groove (Figs. 3E and 5A). This movement, which is initiated at E9.5 and essentially completed by E11.5, leads to a gap in the initially continuous ring of GFP+ cells and thereby to two independent domains of lysozyme expression, one located ventrally and the other dorsally (Figs. 3 and 5). Importantly, X-gal+ cells were absent in the inferior region of the left ventricular free wall in adult LysM ancestry mice as well as in E14.5 embryos (Figs. 1B–D and data not shown). This strongly suggests that the shift in the location of GFP+ cells in the ventral part of the primitive ventricle is caused by cellular movements and not simply by a change in the expression pattern of lysM. Nevertheless, it cannot be ruled out that some of the lysM+ cells present at E9 disappear at later stages, such as by apoptosis. The second step in IVS formation is the movement of lysM+ cells from the bulbo-ventricular groove between E11.5 and E13.5 in a dorsal direction, thereby leading to the closure of the interventricular foramen (Figs. 5B, C). The localization of lysM+ cells to trabeculae in the E10 heart (Figs. 3F–H) and to the outer layers of the IVS at E14.5 (Fig. 6) supports the notion that interventricular septation is achieved, at least in part, by the compaction of trabeculae. This process has been described previously in chicken embryos (Ben-Shachar et al., 1985). Our observation that cardiomyocytes in the outer layer of the IVS maintain lysozyme expression after septation is completed suggests that septal growth is mediated by the continuous addition of trabecular sheets mediates until postnatal stages.

The analysis of adult LysM ancestry mice showed that reporter gene expression preferentially labels the part of the IVS that faces the lumen of the left ventricle (Figs. 1, 2, 8A). This is not an artifact of the reporter system used since the ROSA26 locus is expressed in all parts of the embryonic myocardium (Kitajima et al., 2006). We therefore conclude that the IVS is heterogeneous in origin, deriving predominantly but not exclusively from lysM-positive cardiomyocyte precursors. This conclusion is consistent with the proposition that the myocardium of the IVS originates both from the right and the left ventricular primordium (Franco et al., 2006; Meilhac et al., 2004). In fact, the asymmetrical distribution of reporter labeled cells seen in the septum of adult LysM ancestry mice is anticipated in the embryo, where lysM+ cells are part of the primitive left ventricle (Figs. 3, 5, 8B). This observation suggests that little left to right mixing of myocardial cells occurs during interventricular septation, with the possible exception of X-gal labeled adult cardiomyocytes in the side of the IVS that faces the right ventricle.

In addition to their contribution to the IVS, lysM+ precursors form parts of the left ventricular free wall, especially towards the base of the heart (Figs. 1D, 8A), showing that these two parts of the adult heart are developmentally related. In fact, they can be traced to different domains within the ring of lysM+ cells in the E9 heart (Figs. 3, 5, 8B): while most of the IVS derives

from trabeculae in the ventral part of the primitive left ventricle, the labeled cells in the ventricular free wall most likely originate from the dorsal domain of lysozyme expression. The conclusion that no IVS cardiomyocytes are derived from the dorsal domain is supported by the presence of a buffer of X-gal-negative mesenchymal cells between the X-gal+ cardiomyocytes in the IVS and the region dorsal of the IVS, respectively (Figs. 6C, E). This interpretation supports histological observations suggesting that the region of the outflow tract contributes mesenchymal cells but not muscle cells to the IVS (Kaufman and Bard, 1999).

Possible role of cardiac lysozyme

The specificity of lysM expression during heart development suggests a role for this protein in IVS formation. However, neither homozygous LysM-EGFP nor LysM ancestry mice, which are lysM-deficient, showed any obvious cardiac defects or histological abnormalities (S. Factor and M.S., unpublished observations). The lack of an overt cardiac phenotype might be caused by the expression of lysP in the heart (Fig. 7), a protein that is highly related to lysM and in part rescues the antimicrobial defects seen in lysM-deficient mice (Markart et al., 2004).

The best established role of lysozyme is the hydrolysis of peptidoglycans in the wall of gram-positive bacteria (Masschalck and Michiels, 2003). However, because of the immuno-protected location of the embryo inside the mother, an antimicrobial function of lysozyme expression in IVS precursors appears unlikely. A function of lysozyme in the heart has been described recently. Thus, binding of lysozyme to endocardial endothelial cells activates NO signaling and appears to be involved in cardiac depression during septic shock (Mink et al., 2003). Our finding that lysM+ cardiomyocytes are localized in trabeculae and the outer layers of the myocardium, structures that are in close contact with the endocardium, therefore raises the possibility that lysozyme participates in a cross-talk between endocardium and myocardium during heart development. An alternative, but not mutually exclusive, function is suggested by the observation that lysozyme is first expressed in the trabeculae but then turned off after they compact to form the inner layers of the IVS myocardium (Fig. 6). Thus, lysozyme might play a role during the coalescence of trabeculae. Finally, it cannot be excluded that lysM and lysP, which are contained within a 20-kb region on chromosome 10, have no function in cardiomyocyte precursors and that their expression simply reflects co-regulation with yet another, functionally relevant, gene. While groups of adjacent similarly expressed genes have been described for *Drosophila* (Spellman and Rubin, 2002), the inspection of the mouse genome using the Ensembl database (www.ensemble.org) revealed no gene with a specific cardiac function within 500 kb upstream or downstream of the lysozyme locus (M.S. and T.G., unpublished observation). Our data therefore raise the possibility that animals that lack both lysozyme genes have a cardiac phenotype. However, to our knowledge lysP-deficient mice have not been generated yet.

While lysozyme expression is not maintained in adult cardiomyocytes, lysozyme expressing tissue macrophages are present in the adult heart, especially in the atria and the inner surface of the ventricular chambers. The high abundance of these cells and their alignment along cardiomyocytes are striking (Figs. 2F, G and Suppl. Fig. 2). It will be interesting to determine whether macrophages play a role in the homeostasis of the heart, besides their established functions in the defense against bacteria and the removal of apoptotic cells.

Regulation of cardiac lysM expression

The expression of lysM in macrophages is regulated by myeloid transcription factors such as PU.1 and C/EBPβ (Faust et al., 1999; Lefevre et al., 2003), prompting the question whether the gene is similarly regulated in myocardial precursor cells. This is not the case since LysM ancestry mice lacking PU.1 or C/EBPβ show no reduction of cardiomyocyte labeling (Suppl. Fig. 3). Furthermore, although lysM and lysP are both expressed in the developing heart, only lysM is expressed in bone marrow (Fig. 7). It is therefore likely that there is a distinct transcriptional mechanism that regulates lysozyme expression in the heart.

Since lysozyme expression in the embryonic heart is highly asymmetrical (Fig. 5) it might be controlled by cardiac transcription factors such as Hand1 and Hand2 (McFadden et al., 2005) which define right versus left ventricular identity, or the antagonistic pair Tbx5 and Tbx20, known to be involved in the specification of the IVS (Takeuchi et al., 2003). Additional possible regulators of lysozyme expression are the iroquois-related homeobox genes Irx1 and Irx2, which are expressed in a fashion reminiscent to lysM in the nascent IVS (Christoffels et al., 2000). To determine whether any of these factors are involved in the regulation of cardiac lysozyme expression, and to further define the differences between lysM+ and lysM− myocardial cells, it will be interesting to study the gene expression pattern of IVS precursors isolated from LysM-EGFP embryos.

In conclusion, the combined analysis of LysM-EGFP and LysM ancestry mice has led to the identification of a novel myocardial precursor population and to a description of the dynamics of IVS formation. Based on our observations, LysM-Cre mice should become useful for the specific deletion of genes in the nascent IVS, permitting to probe their function in cardiac septation. Such experiments might shed new light on the molecular basis of ventricular septal defects in humans.

Acknowledgments

We thank Marisa de Andres and Catherine Laiosa for their help with establishing quantitative real-time RT-PCR, Radma Mahmood for the assistance in the preparation of tissue sections, Dan Tenen for providing floxed PU.1 mice and Hilde Ye for the C/EBPβ mice. We are also grateful to Takashi Mikawa and Rick Kitsis for their help in the very early stages of this project as well as to Todd Evans and Lourdes Mendez for their valuable comments on the manuscript. This work was supported by NIH grant RO1 NS43881-01 (T.G.) and by a scholarship from the Boehringer Ingelheim Fonds (M.S.).

Appendix A. Supplementary data

Supplementary data associated with this article can be found, in the online version, at doi:10.1016/j.ydbio.2006.09.025.

References

Balsam, L.B., Wagers, A.J., Christensen, J.L., Kofidis, T., Weissman, I.L., Robbins, R.C., 2004. Haematopoietic stem cells adopt mature haematopoietic fates in ischaemic myocardium. Nature 428, 668–673.

Ben-Shachar, G., Arcilla, R.A., Lucas, R.V., Manasek, F.J., 1985. Ventricular trabeculations in the chick embryo heart and their contribution to ventricular and muscular septal development. Circ. Res. 57, 759–766.

Brodsky, W.Y., Tsirekidze, N.N., Arefyeva, A.M., 1985. Mitotic-cyclic and cycle-independent growth of cardiomyocytes. J. Mol. Cell. Cardiol. 17, 445–455.

Buckingham, M., Meilhac, S., Zaffran, S., 2005. Building the mammalian heart from two sources of myocardial cells. Nat. Rev., Genet. 6, 826–835.

Christoffels, V.M., Keijser, A.G., Houweling, A.C., Clout, D.E., Moorman, A.F., 2000. Patterning the embryonic heart: identification of five mouse Iroquois homeobox genes in the developing heart. Dev. Biol. 224, 263–274.

Clausen, B.E., Burkhardt, C., Reith, W., Renkawitz, R., Forster, I., 1999. Conditional gene targeting in macrophages and granulocytes using LysMcre mice. Transgenic Res. 8, 265–277.

Cross, M., Mangelsdorf, I., Wedel, A., Renkawitz, R., 1988. Mouse lysozyme M gene: isolation, characterization, and expression studies. Proc. Natl. Acad. Sci. U. S. A. 85, 6232–6236.

de la Cruz, M.V., Castillo, M.M., Villavicencio, L., Valencia, A., Moreno-Rodriguez, R.A., 1997. Primitive interventricular septum, its primordium, and its contribution in the definitive interventricular septum: in vivo labelling study in the chick embryo heart. Anat. Rec. 247, 512–520.

Downs, K.M., Davies, T., 1993. Staging of gastrulating mouse embryos by morphological landmarks in the dissecting microscope. Development 118, 1255–1266.

Faust, N., Bonifer, C., Sippel, A.E., 1999. Differential activity of the −2.7 kb chicken lysozyme enhancer in macrophages of different ontogenic origins is regulated by C/EBP and PU.1 transcription factors. DNA Cell Biol. 18, 631–642.

Faust, N., Varas, F., Kelly, L.M., Heck, S., Graf, T., 2000. Insertion of enhanced green fluorescent protein into the lysozyme gene creates mice with green fluorescent granulocytes and macrophages. Blood 96, 719–726.

Franco, D., Meilhac, S.M., Christoffels, V.M., Kispert, A., Buckingham, M., Kelly, R.G., 2006. Left and right ventricular contributions to the formation of the interventricular septum in the mouse heart. Dev. Biol. 294, 366–375.

Habets, P.E., Moorman, A.F., Christoffels, V.M., 2003. Regulatory modules in the developing heart. Cardiovasc. Res. 58, 246–263.

Kaufman, M.H., Bard, J., 1999. The Anatomical Basis of Mouse Development. Academic Press, San Diego.

Kitajima, S., Miyagawa-Tomita, S., Inoue, T., Kanno, J., Saga, Y., 2006. Mesp1-nonexpressing cells contribute to the ventricular cardiac conduction system. Dev. Dyn. 235, 395–402.

Lamers, W.H., Wessels, A., Verbeek, F.J., Moorman, A.F., Viragh, S., Wenink, A.C., Gittenberger-de Groot, A.C., Anderson, R.H., 1992. New findings concerning ventricular septation in the human heart. Implications for maldevelopment. Circulation 86, 1194–1205.

Lefevre, P., Melnik, S., Wilson, N., Riggs, A.D., Bonifer, C., 2003. Developmentally regulated recruitment of transcription factors and chromatin modification activities to chicken lysozyme cis-regulatory elements in vivo. Mol. Cell. Biol. 23, 4386–4400.

Lichanska, A.M., Browne, C.M., Henkel, G.W., Murphy, K.M., Ostrowski, M.C., McKercher, S.R., Maki, R.A., Hume, D.A., 1999. Differentiation of the mononuclear phagocyte system during mouse embryogenesis: the role of transcription factor PU.1. Blood 94, 127–138.

Markart, P., Faust, N., Graf, T., Na, C.L., Weaver, T.E., Akinbi, H.T., 2004. Comparison of the microbicidal and muramidase activities of mouse lysozyme M and P. Biochem. J. 380, 385–392.

Masschalck, B., Michiels, C.W., 2003. Antimicrobial properties of lysozyme in relation to foodborne vegetative bacteria. Crit. Rev. Microbiol. 29, 191–214.

McFadden, D.G., Barbosa, A.C., Richardson, J.A., Schneider, M.D., Srivastava, D., Olson, E.N., 2005. The Hand1 and Hand2 transcription factors regulate expansion of the embryonic cardiac ventricles in a gene dosage-dependent manner. Development 132, 189–201.

McGrath, K.E., Koniski, A.D., Malik, J., Palis, J., 2003. Circulation is established in a stepwise pattern in the mammalian embryo. Blood 101, 1669–1676.

Meilhac, S.M., Esner, M., Kerszberg, M., Moss, J.E., Buckingham, M.E., 2004. Oriented clonal cell growth in the developing mouse myocardium underlies cardiac morphogenesis. J. Cell Biol. 164, 97–109.

Mink, S.N., Jacobs, H., Bose, D., Duke, K., Cheng, Z.Q., Liu, G., Light, R.B., 2003. Lysozyme: a mediator of myocardial depression and adrenergic dysfunction in septic shock in dogs. J. Mol. Cell. Cardiol. 35, 265–275.

Moorman, A.F., Christoffels, V.M., 2003. Cardiac chamber formation: development, genes, and evolution. Physiol. Rev. 83, 1223–1267.

Murry, C.E., Soonpaa, M.H., Reinecke, H., Nakajima, H., Nakajima, H.O., Rubart, M., Pasumarthi, K.B., Virag, J.I., Bartelmez, S.H., Poppa, V., Bradford, G., Dowell, J.D., Williams, D.A., Field, L.J., 2004. Haematopoietic stem cells do not transdifferentiate into cardiac myocytes in myocardial infarcts. Nature 428, 664–668.

Nagasawa, T., Hirota, S., Tachibana, K., Takakura, N., Nishikawa, S., Kitamura, Y., Yoshida, N., Kikutani, H., Kishimoto, T., 1996. Defects of B-cell lymphopoiesis and bone-marrow myelopoiesis in mice lacking the CXC chemokine PBSF/SDF-1. Nature 382, 635–638.

Orlic, D., Kajstura, J., Chimenti, S., Jakoniuk, I., Anderson, S.M., Li, B., Pickel, J., McKay, R., Nadal-Ginard, B., Bodine, D.M., Leri, A., Anversa, P., 2001. Bone marrow cells regenerate infarcted myocardium. Nature 410, 701–705.

Parlakian, A., Tuil, D., Hamard, G., Tavernier, G., Hentzen, D., Concordet, J.P., Paulin, D., Li, Z., Daegelen, D., 2004. Targeted inactivation of serum response factor in the developing heart results in myocardial defects and embryonic lethality. Mol. Cell. Biol. 24, 5281–5289.

Rehm, S., Devor, D.E., Henneman, J.R., Ward, J.M., 1991. Origin of spontaneous and transplacentally induced mouse lung tumors from alveolar type II cells. Exp. Lung Res. 17, 181–195.

Rentschler, S., Vaidya, D.M., Tamaddon, H., Degenhardt, K., Sassoon, D., Morley, G.E., Jalife, J., Fishman, G.I., 2001. Visualization and functional characterization of the developing murine cardiac conduction system. Development 128, 1785–1792.

Soriano, P., 1999. Generalized lacZ expression with the ROSA26 Cre reporter strain. Nat. Genet. 21, 70–71.

Spellman, P.T., Rubin, G.M., 2002. Evidence for large domains of similarly expressed genes in the *Drosophila* genome. J. Biol. 1, 5.

Srinivas, S., Watanabe, T., Lin, C.S., William, C.M., Tanabe, Y., Jessell, T.M., Costantini, F., 2001. Cre reporter strains produced by targeted insertion of EYFP and ECFP into the ROSA26 locus. BMC Dev. Biol. 1, 4.

Stadtfeld, M., Graf, T., 2005. Assessing the role of hematopoietic plasticity for endothelial and hepatocyte development by non-invasive lineage tracing. Development 132, 203–213.

Sterneck, E., Tessarollo, L., Johnson, P.F., 1997. An essential role for C/EBPbeta in female reproduction. Genes Dev. 11, 2153–2162.

Tachibana, K., Hirota, S., Iizasa, H., Yoshida, H., Kawabata, K., Kataoka, Y., Kitamura, Y., Matsushima, K., Yoshida, N., Nishikawa, S., Kishimoto, T., Nagasawa, T., 1998. The chemokine receptor CXCR4 is essential for vascularization of the gastrointestinal tract. Nature 393, 591–594.

Takeuchi, J.K., Ohgi, M., Koshiba-Takeuchi, K., Shiratori, H., Sakaki, I., Ogura, K., Saijoh, Y., Ogura, T., 2003. Tbx5 specifies the left/right ventricles and ventricular septum position during cardiogenesis. Development 130, 5953–5964.

Vaughan, C.J., Basson, C.T., 2000. Molecular determinants of atrial and ventricular septal defects and patent ductus arteriosus. Am. J. Med. Genet. 97, 304–309.

Verzi, M.P., McCulley, D.J., De Val, S., Dodou, E., Black, B.L., 2005. The right ventricle, outflow tract, and ventricular septum comprise a restricted expression domain within the secondary/anterior heart field. Dev. Biol. 287, 134–145.

Wessels, A., Vermeulen, J.L., Verbeek, F.J., Viragh, S., Kalman, F., Lamers, W.H., Moorman, A.F., 1992. Spatial distribution of “tissue-specific” antigens in the developing human heart and skeletal muscle: III. An immunohistochemical analysis of the distribution of the neural tissue

antigen G1N2 in the embryonic heart; implications for the development of the atrioventricular conduction system. Anat. Rec. 232, 97–111.

Ye, M., Iwasaki, H., Laiosa, C.V., Stadtfeld, M., Xie, H., Heck, S., Clausen, B., Akashi, K., Graf, T., 2003. Hematopoietic stem cells expressing the myeloid lysozyme gene retain long-term, multilineage repopulation potential. Immunity 19, 689–699.

Ye, M., Ermakova, O., Graf, T., 2005. PU.1 is not strictly required for B cell development and its absence induces a B-2 to B-1 cell switch. J. Exp. Med. 202, 1411–1422.

Zou, Y.R., Kottmann, A.H., Kuroda, M., Taniuchi, I., Littman, D.R., 1998. Function of the chemokine receptor CXCR4 in haematopoiesis and in cerebellar development. Nature 393, 595–599.